

KRITTIKA SUMMER PROJECTS 2024

Radio Astronomy

Manit Jhajharia

KRITTIKA SUMMER PROJECTS 2024

Radio Astronomy

Manit Jhajharia¹

¹IIT Bombay

Copyright © 2024 Krittika IITB
PUBLISHED BY KRITTIKA: THE ASTRONOMY CLUB OF IIT BOMBAY
[GITHUB.COM/KRITTIKAIITB](https://github.com/KRITTIKAIITB)
Sample Repository: Type project name
First Release, August 2024

Abstract

This report presents an overview of the fundamental principles and methodologies in radio astronomy, as covered in the initial chapters of "Fundamentals of Radio Astronomy: Observational Methods". Chapter 1 introduces the basics of radio astronomy, focusing on the nature of radio waves, their interaction with the interstellar medium, and the electromagnetic spectrum. Chapter 2 delves into radiation physics, detailing the processes that generate radio emissions, including thermal and non-thermal mechanisms. This chapter also emphasizes the significance of spectral line observations, notably the 21 cm line, for probing hydrogen in the galaxy. Chapter 3.1 outlines the design and function of single-dish radio telescopes, exploring their key components, sensitivity, and resolution capabilities. It discusses the role of antenna systems and receivers in capturing and amplifying weak radio signals. Chapter 3.3 addresses the complexities of data collection and processing, highlighting techniques for reducing noise and improving signal clarity through calibration and signal integration methods. The report aims to elucidate the essential concepts and practical aspects of radio astronomy, laying the groundwork for advanced observational techniques and research applications.

Contents

I

Week 1

1	Theory	9
1.1	Introduction to Radio Astronomy and Radio Physics	9
1.2	Fundamentals of Radio Waves	9
1.2.1	Electromagnetic Spectrum and Radio Waves	10
1.2.2	Spectroscopy and Applications in Radio Astronomy	10
1.3	Understanding the Sky Coordinate System and Observer-Centered Definitions	10
1.3.1	Sky Coordinate System	10
1.3.2	Observer-Centered Definitions	10
1.3.3	Meridian and Transit	11
1.3.4	Apparent Sizes and Solid Angles	11
1.4	Basic Structure of a Traditional Radio Telescope	11
1.4.1	Basic Structure	11
1.4.2	Atmospheric Transparency	12
1.4.3	Resolution and Sensitivity	12
1.4.4	Data Handling	12
2	Work	13
2.1	Multi-Wavelength Astronomy	13
2.2	Plotting The Jet Afterglow Lightcurve Of GW170817	13

II

Week 2

1	Theory	17
1.1	Blackbody Radiation and its Physical Characteristics	17
1.2	Planck Function	17
1.2.1	Stefan–Boltzmann Law	17
1.2.2	Wien’s Displacement Law	18
1.2.3	Rayleigh–Jeans Approximation	18
1.2.4	Brightness Temperature	18
1.3	Coherent and Incoherent Radiation	19
1.4	Interference	19
1.4.1	Interference Patterns	19
1.4.2	Applications	20
1.5	Polarization of Radiation	20
1.5.1	Types of Polarization	20
1.5.2	Measurement of Polarization	20
2	Work	21
2.1	Finding the Temperature of the Cosmic Microwave Background(CMB)	21
2.2	Plotting the Galaxy Rotation Curve	22

III

Week3

1	Theory	27
1.1	Radio Telescope Reflectors, Antennas, and Feeds	27
1.2	Primary Reflectors	27
1.2.1	Diffraction and Beam Pattern	28
1.2.2	Resolution and Directivity	28
1.3	Feeds and Primary Reflector Illumination	28
1.4	Surface Errors	29
1.5	Beam Pattern	29
1.6	Noise, Noise Temperature, and Antenna Temperature	29
1.6.1	Impact on Telescope Performance	29

IV

Week5

1	Theory	33
1.1	CASA	33
1.1.1	Key Uses of CASA:	33
1.1.2	t clean	33
1.1.3	imfit	34
1.1.4	imstat	34

1.2	CARTA	34
1.2.1	Key Features of CARTA	35
2	Work	37
2.1	Taking a look at the data	37
2.2	Using tclean	38
2.2.1	Post cleaning	38
2.2.2	Changing weighting scheme	38
2.2.3	Tweaking calibrators	39
2.2.4	Using big pixel size	39

V

Week6

1	Theory	43
1.1	Introduction to MCMC	43
1.2	Key Points	43
1.2.1	Introduction to MCMC	43
1.2.2	Basic Concepts	43
1.2.3	Bayesian Inference	43
1.2.4	Common MCMC Algorithms	44
1.2.5	Practical Implementation	44
1.2.6	Applications and Examples	44
1.2.7	Diagnostic Tools	44
1.2.8	Software and Tools	44
2	Work	45
2.1	Practice Problems	45

VI

Week7

1	Work	51
1.1	Introduction	51
1.2	Initial Implementation: Custom MCMC Sampler	51
1.2.1	Methodology	51
1.2.2	Challenges	52
1.3	Advanced Implementation: Using emcee	52
1.3.1	Methodology	52
1.3.2	Challenges and Improvements	52
1.3.3	Outcomes	53
1.4	Conclusion	53
1.5	Results	53
	Bibliography	55
	Books	55



Week 1

1	Theory	9
1.1	Introduction to Radio Astronomy and Radio Physics	
1.2	Fundamentals of Radio Waves	
1.3	Understanding the Sky Coordinate System and Observer-Centered Definitions	
1.4	Basic Structure of a Traditional Radio Telescope	
2	Work	13
2.1	Multi-Wavelength Astronomy	
2.2	Plotting The Jet Afterglow Lightcurve Of GW170817	



1. Theory

1.1 Introduction to Radio Astronomy and Radio Physics

(1) This report explores key concepts from "Fundamentals of Radio Astronomy: Observational Methods" by Marr, Snell, and Kurtz, focusing on chapters 1, 2, and sections 3.1 and 3.3.

- Chapter 1 introduces the development and impact of radio astronomy. It covers the discovery of cosmic radio waves and the evolution of radio telescopes, emphasizing their role in studying phenomena like the cosmic microwave background and pulsars.
- Chapter 2 delves into radiation physics, explaining electromagnetic radiation, blackbody radiation, and spectral lines. It discusses emission mechanisms such as synchrotron and thermal radiation, which are crucial for interpreting radio signals from astronomical sources.
- Sections 3.1 and 3.3 provide an in-depth look at radio telescopes and observational techniques. They explain the components and operation of radio telescopes, including antennas, receivers, and feed systems, and introduce key concepts like beamwidth, sensitivity, and resolution. These sections also cover single-dish radio telescope observations, detailing methodologies for mapping the sky, measuring radio sources, and calibrating observations. Practical aspects such as noise reduction and correction for atmospheric effects are discussed, highlighting the capabilities and limitations of single-dish observations.

1.2 Fundamentals of Radio Waves

Radio waves are a type of electromagnetic radiation with lower frequencies than visible light. They consist of oscillating electric and magnetic fields perpendicular to their direction of travel, moving at a constant speed c (approximately $3.00 \times 10^8 \text{ m/s}$). Their wavelength λ and frequency v are related by $\lambda v = c$.

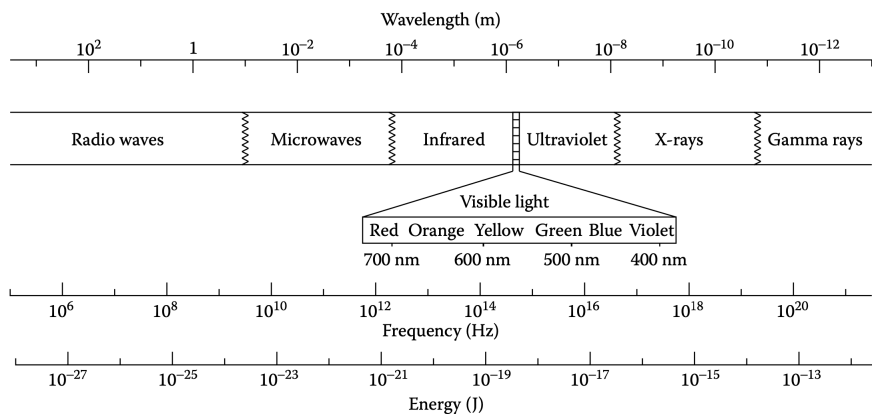


Figure 1.1: Display of all the bands of the entire electromagnetic spectrum, shown in order of energy of the waves, with the lowest energy radiation on the left.

1.2.1 Electromagnetic Spectrum and Radio Waves

Radio waves span from 10 MHz to 300 GHz on the electromagnetic spectrum, known as the "radio window." They penetrate Earth's atmosphere, allowing ground-based radio observations.

1.2.2 Spectroscopy and Applications in Radio Astronomy

Spectroscopy is pivotal in radio astronomy, analyzing spectra—continuous or with emission/absorption lines—to unveil details about celestial sources.

Radio telescopes detect and analyze radio waves from space, enabling studies of cosmic microwave background radiation, pulsars, and molecular clouds. They extend observational capabilities beyond optical telescopes.

1.3 Understanding the Sky Coordinate System and Observer-Centered Definitions

1.3.1 Sky Coordinate System

- **Right Ascension (RA):** Measured in hours, minutes, and seconds, RA lines are fixed relative to the stars, aligning initially with Earth's longitude on the vernal equinox. RA increases to the east due to Earth's rotation.
- **Declination (Dec):** Analogous to latitude, Dec is measured in degrees north or south from the celestial equator. It remains constant relative to the stars as Earth rotates.

1.3.2 Observer-Centered Definitions

- **Horizon:** Defines the visible sky from a specific location, obstructed by Earth's surface.
- **Zenith:** Directly overhead point in the sky, continuously changing due to Earth's rotation.
- **Altitude:** Angular height of an object above the horizon, varying from 0° (on horizon) to 90° (zenith).
- **Azimuth:** Angular position of an object along the horizon, referenced from due north (0°), east (90°), south (180°), and west (270°).

1.3.3 Meridian and Transit

- **Meridian:** Line in the sky passing through zenith and celestial poles.
- **Transit:** Occurs when an object passes through the observer's meridian, indicating its highest point in the sky.
- **Hour Angle (HA):** Time since an object's transit, useful for scheduling observations.
- **Local Sidereal Time (LST):** RA of the meridian, aiding in tracking when objects transit based on their RA.

1.3.4 Apparent Sizes and Solid Angles

- **Angular Size:** Describes how large an object appears in the sky, measured in radians.
- **Solid Angle:** Extension of angular size to a three-dimensional space, critical for understanding an object's visibility.
- **Steradians (sr):** Unit measuring solid angles, with the entire sky covering 4 steradians.

1.4 Basic Structure of a Traditional Radio Telescope

Radio astronomy involves observing celestial objects at radio wavelengths using specialized instruments known as radio telescopes. Unlike visible light telescopes, radio telescopes detect electromagnetic radiation at much longer wavelengths, which requires different technological approaches and observing conditions. This section provides an overview of the basic components and operational principles of a traditional radio telescope based on the text provided.

1.4.1 Basic Structure

1. Parabolic Reflector (Dish):

1. The primary component of a radio telescope is the parabolic reflector or dish, which collects and focuses radio waves. Unlike visible light telescopes that use lenses, radio telescopes rely on reflecting surfaces due to the properties of radio waves.
2. The size of the dish determines the sensitivity of the telescope, directly affecting its ability to capture faint radio signals from celestial sources.
3. At longer radio wavelengths, the dish can even be a mesh structure rather than a solid surface, provided the mesh holes are smaller than the wavelength being observed.

Mount:

mount is the physical structure that supports and moves the dish. Most modern radio telescopes use an Altitude-Azimuth (Alt-Az) mount, which allows movement in altitude (up-down) and azimuth (side-to-side). Older equatorial mounts are also used, tilted to align with the Earth's rotational axis, translating movement into Right Ascension (RA) and Declination (Dec) coordinates.

Feed, Receivers, and Computers:

1. Radio waves collected by the dish are directed to a feed antenna, which converts the waves into electrical signals.

2. These signals are then processed by a receiver front-end located near the feed, amplifying and converting the signal to a manageable frequency range.
3. The processed signal is transmitted via coaxial cable to the receiver back-end, which further detects and digitizes the signal for analysis by a computer.
4. Each feed-receiver assembly typically corresponds to a single detector, akin to a pixel in imaging systems.

Observational Considerations

1.4.2 Atmospheric Transparency

: Unlike visible light, radio waves are not significantly scattered by Earth's atmosphere. This allows radio observations to be conducted during both day and night, as well as under cloudy conditions at longer wavelengths.

1.4.3 Resolution and Sensitivity

: The resolution of a radio telescope is determined by diffraction rather than atmospheric turbulence, with larger dishes providing better angular resolution.

1.4.4 Data Handling

: Radio astronomy data differs from visible light observations in that it typically results in fewer discrete measurements per observation, emphasizing precision over spatial coverage.

2. Work

2.1 Multi-Wavelength Astronomy

we will choose interesting portions of the sky and compare the images from different telescopes to see how astrophysical objects differ in their emission at different wavelengths.

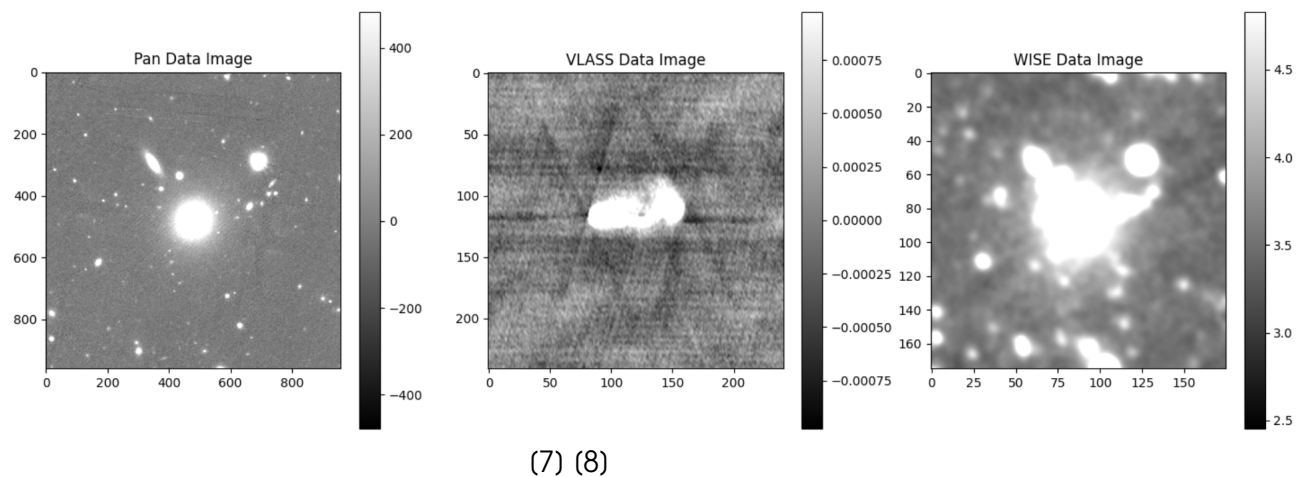


Figure 2.1: Figure obtained upon pre-processing and removing outliers from the image data

2.2 Plotting The Jet Afterglow Lightcurve Of GW170817

We get the data from VLA telescope with frequency of 3GHz and the data of Chandra telescope with frequency of 2.41×10^{17} Hz, and converting the 2.41×10^{17} Hz data to 3 GHz data, with the relation $F_v \propto v^{-0.584}$. (5)

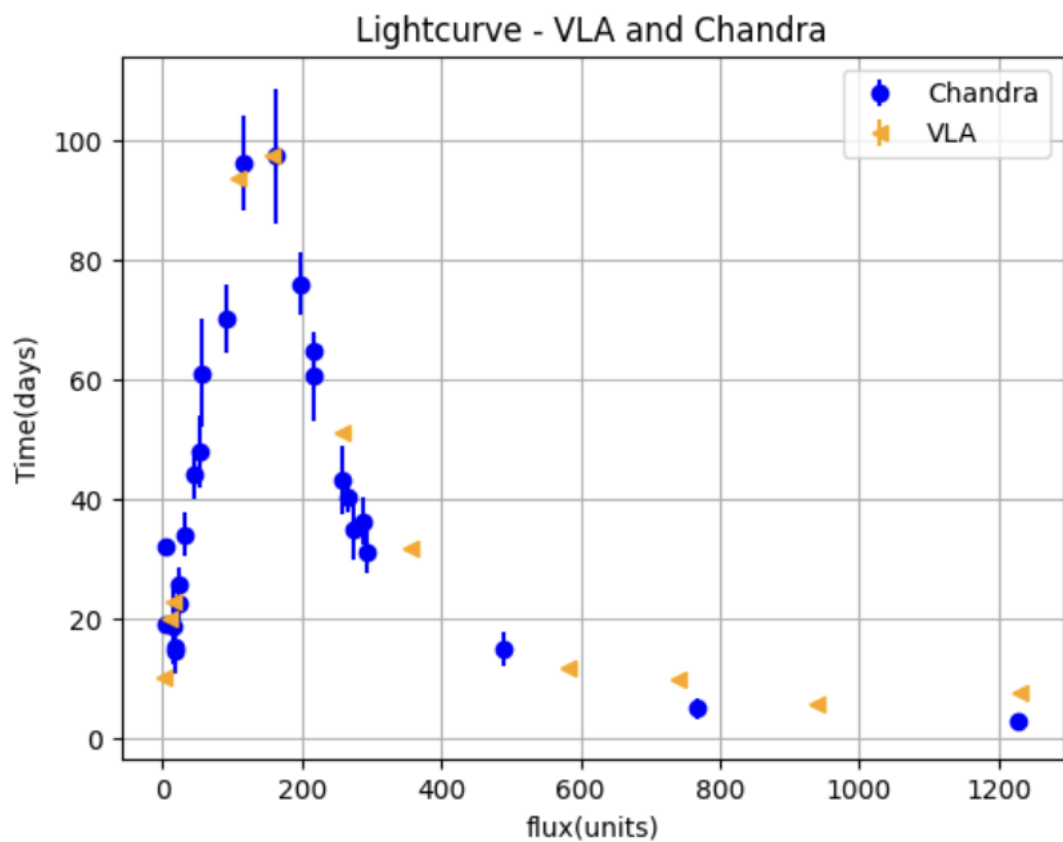
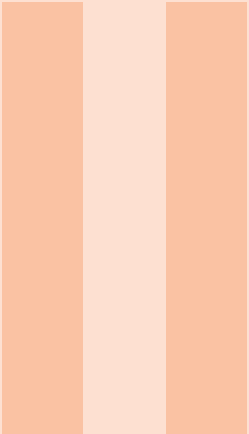


Figure 2.2: Plotting the data points of Chandra and VLA



Week 2

1	Theory	17
1.1	Blackbody Radiation and its Physical Characteristics	
1.2	Planck Function	
1.3	Coherent and Incoherent Radiation	
1.4	Interference	
1.5	Polarization of Radiation	
2	Work	21
2.1	Finding the Temperature of the Cosmic Microwave Background(CMB)	
2.2	Plotting the Galaxy Rotation Curve	

1. Theory

1.1 Blackbody Radiation and its Physical Characteristics

(2)

Blackbody radiation refers to the thermal radiation emitted by an idealized object that absorbs all incident light and reflects none. This theoretical concept helps in understanding how objects emit and absorb radiation based on their temperature. The intensity of blackbody radiation across different frequencies is described by the Planck function, which depends solely on the body's temperature and the frequency of the emitted radiation.

1.2 Planck Function

The Planck function, $B_v(T)$, characterizes the spectral intensity of blackbody radiation per unit frequency interval per unit solid angle. It is expressed as:

$$B_v(T) = \frac{2hv^3}{c^2} \frac{1}{\exp(\frac{hv}{kT}) - 1}$$

where:

- h is Planck's constant,
- v is the frequency of the radiation,
- k is Boltzmann's constant,
- T is the temperature of the radiating body,
- c is the speed of light.

1.2.1 Stefan–Boltzmann Law

The total flux of radiation emitted by a blackbody is proportional to the fourth power of its temperature, as described by the Stefan–Boltzmann law:

$$F = \sigma T^4$$

where σ is the Stefan–Boltzmann constant.

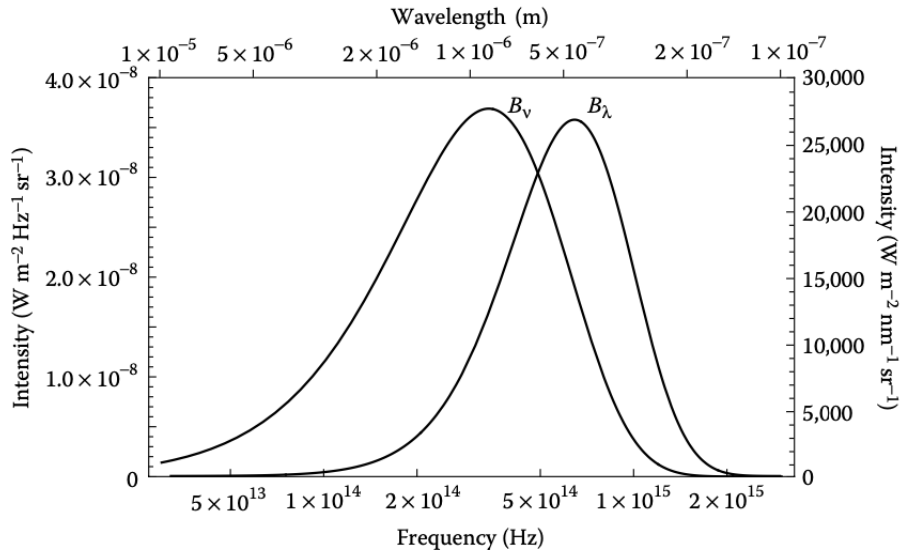


Figure 1.1: Curves of the Planck function for a 5800 K blackbody shown as both B_λ and B_ν . Even though both of these curves represent the intensity emitted by the same blackbody, they peak in different parts of the electromagnetic spectrum.

1.2.2 Wien's Displacement Law

Wien's displacement law states that the wavelength at which the emission spectrum of a blackbody peaks is inversely proportional to its temperature:

$$\lambda_{\text{peak}} T = b$$

where b is a constant.

1.2.3 Rayleigh–Jeans Approximation

At lower frequencies or longer wavelengths (e.g., in the radio region), the Planck function simplifies to the Rayleigh–Jeans approximation:

$$B_\nu(T) \approx \frac{2kT\nu^2}{c^2}$$

This approximation is valid when $h\nu \ll kT$.

1.2.4 Brightness Temperature

Brightness temperature (T_B) is a parameter used in radio astronomy to describe the intensity of radiation from a source. It represents the temperature of a hypothetical blackbody that would emit radiation at the same intensity observed:

$$T_B = \frac{c^2}{2k\nu^2} I_\nu$$

where I_ν is the intensity of the radiation.

1.3 Coherent and Incoherent Radiation

The concept of coherence in electromagnetic radiation plays a crucial role in understanding its properties and applications, especially in fields like radio astronomy. Coherent radiation refers to waves that maintain a constant phase relationship over time and space, whereas incoherent radiation consists of waves with random phases.

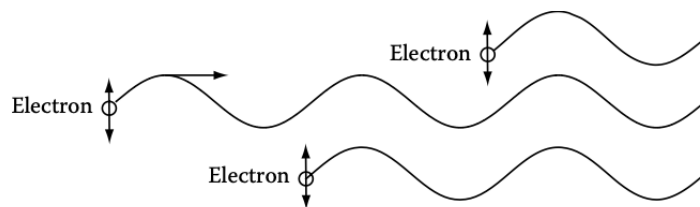


Figure 1.2: Schematic of the creation of coherent radiation. An oscillating electron emits a chain of sine waves, which is joined by another identical chain of sine waves with exactly the same phase, and then another wave is added, in phase with the first two.

1. Coherent Radiation:

Definition : Radiation where all wave components have a fixed phase relationship.

Properties : Results in constructive interference, amplifying the intensity significantly. Examples include lasers and some astronomical sources.

Mathematical Representation : The addition of coherent waves leads to an intensity that can be several times higher than the sum of individual wave intensities, depending on the phase relationship.

2. Incoherent Radiation:

Definition : Radiation from sources where wave components have random phases.

Properties : Results in overall intensity proportional to the sum of individual intensities. Typical examples include thermal sources like incandescent bulbs and most astronomical sources.

1.4 Interference

1.4.1 Interference Patterns

: Illustrated by the double-slit experiment, where coherent light sources produce distinct interference patterns due to phase differences.

1.4.2 Applications

: Understanding interference patterns helps in designing radio telescopes and interferometers. Even partially coherent sources can produce interference patterns, impacting observational techniques in radio astronomy.

1.5 Polarization of Radiation

Electromagnetic waves propagate with mutually perpendicular electric and magnetic fields perpendicular to the direction of propagation. Polarization refers to the orientation of the electric field vector of these waves. In the context of radio astronomy, understanding polarization helps discern physical properties of astronomical sources.

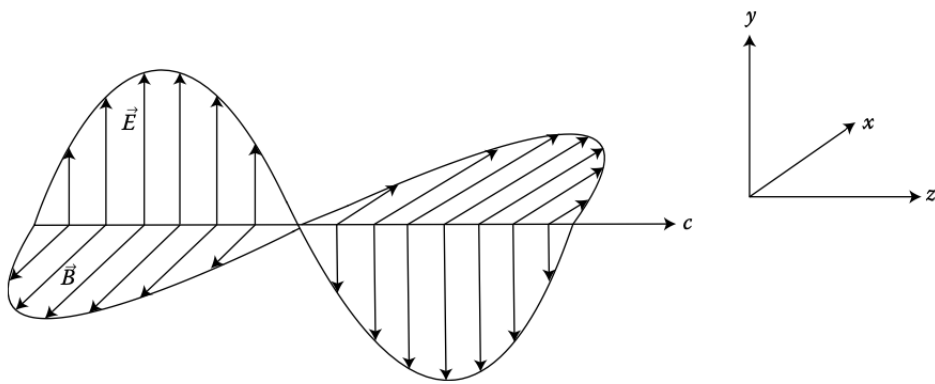


Figure 1.3: Propagation of plane electromagnetic waves along the z-axis with the electric field oscillating along the y-axis.

1.5.1 Types of Polarization

- Linear Polarization: The electric field oscillates in a single plane.
- Circular Polarization: The electric field vector rotates either clockwise or counterclockwise as the wave propagates.
- Elliptical Polarization: The electric field vector traces out an elliptical path due to varying magnitudes and phases of its components.

1.5.2 Measurement of Polarization

Polarization is quantitatively described using Stokes parameters, which provide a comprehensive framework to measure both linear and circular polarization simultaneously.

Stokes Parameters

Stokes I (Total Intensity) : Sum of intensities of orthogonal polarizations.

Stokes Q and U (Linear Polarization) : Measure the difference and correlation between two orthogonal linear polarization states.

Stokes V (Circular Polarization) : Measures the difference between intensities of left and right circular polarization.

2. Work

2.1 Finding the Temperature of the Cosmic Microwave Background(CMB)

The Cosmic Microwave Background (CMB) is a relic of the Big Bang that allows astronomers to probe the universe at an age as young as 400,000 years. When measured at different frequencies, we can know more about the nature of this radiation. In this activity, we used far infrared data adapted from the COBE satellite to fit a blackbody curve to the CMB.

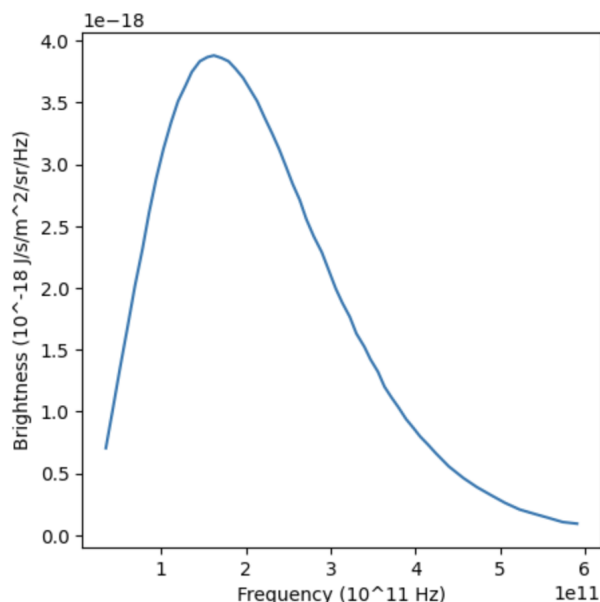


Figure 2.1: Plotting the Frequency vs Brightness

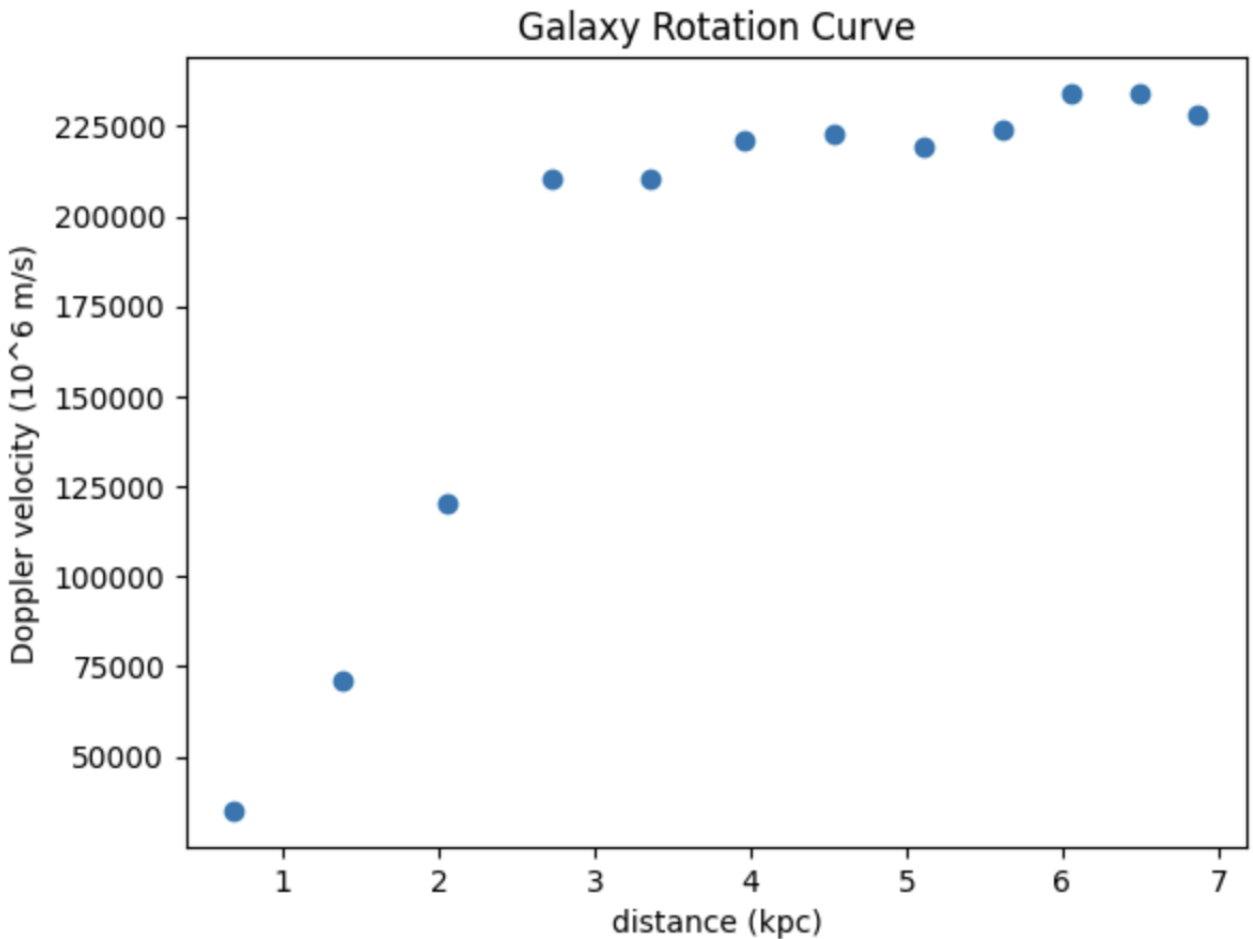
Knowing that it is a blackbody spectrum, we fit the blackbody function to the data with temperature as the free parameter. We end up getting

$$T_{CMB} = 2.740289273966668K$$

The expansion of the Universe has stretched out the CMB radiation by around 1000 times, which makes it look much cooler. So instead of seeing the afterglow at around 3000 degrees, we see it at just 30 above absolute zero, or 3 Kelvin (-270°C).

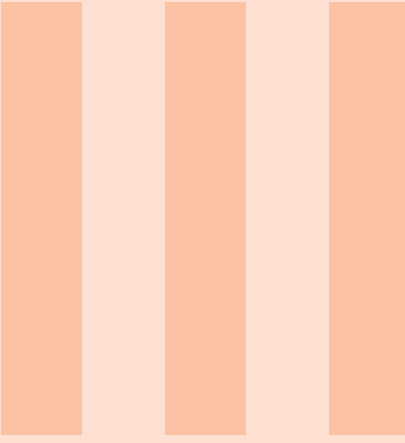
2.2 Plotting the Galaxy Rotation Curve

Fit for the Doppler velocity of the 21 cm line for each distance. To do so, we fit a gaussian to the spectral line and determine the central frequency, we plot the velocities as a function of distance from the centre of our galaxy.



When studying other galaxies it is invariably found that the stellar rotational velocity remains constant, or "flat", with increasing distance away from the galactic center. This result is highly counter-intuitive since, based on Newton's law of gravity, the rotational velocity would steadily decrease for stars further away from the galactic center. Analogously, inner planets within the Solar System travel more quickly about the Sun than

do the outer planets (e.g. the Earth travels around the sun at about 100,000 km/hr while Saturn, which is further out, travels at only one third this speed). One way to speed up the outer planets would be to add more mass to the solar system, between the planets. By the same argument the flat galactic rotation curves seem to suggest that each galaxy is surrounded by significant amounts of dark matter. It has been postulated, and generally accepted, that the dark matter would have to be located in a massive, roughly spherical halo enshrouding each galaxy.



Week3

1	Theory	27
1.1	Radio Telescope Reflectors, Antennas, and Feeds	
1.2	Primary Reflectors	
1.3	Feeds and Primary Reflector Illumination	
1.4	Surface Errors	
1.5	Beam Pattern	
1.6	Noise, Noise Temperature, and Antenna Temperature	



1. Theory

1.1 Radio Telescope Reflectors, Antennas, and Feeds

(3)

In radio telescopes, the terms "antenna" and "reflector" are often used interchangeably but they have distinct meanings. An *antenna* is a device that couples electromagnetic (EM) waves from free space into a transmission line. A *reflector*, typically parabolic, collects and concentrates radiation. Large radio telescopes use a reflector as the initial element, directing EM waves to an antenna that then transmits these waves to the receiver. For long radio wavelengths, simple dipole antennas can act as the primary element.

Dish refers to the reflector, while *feed* denotes the device that couples concentrated radiation into a transmission line.

1.2 Primary Reflectors

Parabolic Reflectors : Most radio telescope dishes are parabolic, ensuring that incoming plane waves (from astronomical objects) are focused to a single point, called the focus. When the source is off the central axis, waves converge to a point near this focus, forming a focal plane. In radio telescopes, the feed horns placed at this focal plane convert EM waves from free space into transmission lines.

Prime Focus Telescopes : In these telescopes, the feed and receivers are at the primary reflector's focus. Multiple feeds may collect power from different directions simultaneously. This setup can be inconvenient due to the awkward placement of feeds and receivers.

Cassegrain Telescopes : A secondary reflector is used to redirect waves to another focal point, often behind the primary reflector. This design is more practical as the feed and receiver are more accessible.

The Green Bank 20-m telescope is an example of a Cassegrain telescope.

Functions of Primary Reflector :

- (a) Collecting and Focusing Radiation: This enhances the detection of faint sources. The collected power depends on the telescope's effective area (A_{eff}), which is smaller than its geometrical area due to several factors.
- (b) Providing Directivity: This enables the telescope to differentiate emissions from objects at different sky positions. The directivity is described by the beam pattern, which is influenced by diffraction.

1.2.1 Diffraction and Beam Pattern

: The beam pattern measures the telescope's sensitivity to incoming signals at various angles, similar to the point-spread function in optical astronomy. The *Huygens-Fresnel principle* illustrates how waves diffract and interfere, forming a beam pattern. The *Airypattern* is a typical sensitivity pattern of a parabolic reflector, with a central peak and sidelobes, determining the telescope's resolution and ability to distinguish closely spaced sources.

1.2.2 Resolution and Directivity

: The resolution angle, defined as the full width at half maximum (FWHM) of the main lobe, indicates the telescope's ability to discern fine details. This angle is inversely proportional to the reflector's diameter, meaning larger telescopes offer better resolution and power collection.

1.3 Feeds and Primary Reflector Illumination

Feeds : At the focal point, antennas (usually horn antennas) couple EM waves into transmission lines leading to receivers. Horn antennas, which may have rectangular or circular cross-sections, are designed to collect and direct waves effectively. The feed horn's beam pattern, determining the illumination on the primary reflector, is crucial for telescope performance.

Illumination Pattern : The illumination pattern affects the telescope's angular resolution, sidelobe sensitivity, and effective collecting area. The ideal pattern maximizes the use of the reflector's area while minimizing background noise.

Edge Taper : This describes the sensitivity ratio between the center and edge of the reflector, influenced by the feed horn's beam width. A large edge taper reduces sensitivity to the reflector's edges, improving sidelobe levels but reducing effective area. A small edge taper improves resolution but increases sidelobes.

1.4 Surface Errors

The primary reflector of a radio telescope is crucial for gathering incoming radio waves. Ideally, it should be a perfect parabola to focus waves precisely. However, manufacturing imperfections lead to deviations from this ideal shape, characterized by root mean square (rms) deviations (δz). These deviations cause phase errors, which reduce the telescope's sensitivity. The Ruze equation quantifies this reduction in collecting area due to surface errors:

$$A_\delta = A_0 e^{-\left(\frac{4\pi\delta z}{\lambda}\right)^2}$$

where A_δ and A_0 are the collecting areas with and without surface errors, respectively. Surface errors should ideally be less than 1/20th of the wavelength of light to minimize performance loss.

1.5 Beam Pattern

The beam pattern of a radio telescope is determined by its aperture and is crucial for understanding its resolution and sensitivity. The pattern is derived using Fourier transforms, relating the electric field distribution across the aperture to its angular distribution in the far-field. For example, a uniformly illuminated aperture yields a beam pattern characterized by a sinc function, with the angular resolution $\theta_{FWHM} = 0.89\lambda/a$ radians.

1.6 Noise, Noise Temperature, and Antenna Temperature

(4)

Noise in radio telescopes originates from internal electronic components and degrades signal detection. The noise temperature (TN) quantifies this noise power in terms of an equivalent temperature. It is critical to minimize TN to enhance sensitivity. The total noise temperature of a receiver chain is the sum of individual noise temperatures weighted by their gains. The total noise temperature TN is given by:

$$TN = \frac{TN_1}{G_1} + \frac{TN_2}{G_1 G_2} + \frac{TN_3}{G_1 G_2 G_3} + \dots$$

1.6.1 Impact on Telescope Performance

Surface errors reduce the effective collecting area, while noise limits the telescope's ability to detect faint astronomical signals. Techniques such as switched power measurements mitigate noise influence but do not eliminate it entirely, emphasizing the need for low-noise components and careful system design.

Week5

IV

1	Theory	33
1.1	CASA	
1.2	CARTA	
2	Work	37
2.1	Taking a look at the data	
2.2	Using <code>tclean</code>	

1. Theory

1.1 CASA

CASA (Common Astronomy Software Applications) is a software suite used primarily for the processing and analysis of radio astronomy data. Developed by the National Radio Astronomy Observatory (NRAO), CASA is widely used by astronomers for its powerful tools that handle data from radio telescopes such as the Very Large Array (VLA) and the Atacama Large Millimeter/submillimeter Array (ALMA).

1.1.1 Key Uses of CASA:

- Data Calibration: CASA provides tools to calibrate raw data collected from radio telescopes, correcting for instrumental and atmospheric effects.
- Imaging: It converts calibrated data into images of the sky, allowing astronomers to visualize celestial phenomena.
- Data Analysis: CASA offers a suite of tools for analyzing astronomical data, including spectral line analysis and polarimetry.
- Simulation: The software can simulate observations, helping astronomers plan their observations and test their analysis methods.
- Scripting and Automation: CASA supports scripting in Python, enabling users to automate repetitive tasks and customize their data processing workflows.

1.1.2 `t clean`

`tclean` is a task in CASA used for image synthesis and deconvolution. This task processes raw visibility data from radio telescopes to produce high-quality images of the sky. Here's a breakdown of what it does:

Image Synthesis Converts raw visibility data into a preliminary image using Fourier transforms. (Deconvolution) Corrects for the blurring effects of the telescope's point spread function (PSF) to produce a clearer image. This involves algorithms like CLEAN, Multi-Scale CLEAN, and others.

Interactive Mode Allows astronomers to interactively refine the image by manually identifying areas of interest for more focused deconvolution.

Spectral and Polarization Imaging Supports creating images across different frequencies (spectral cubes) and polarization states.

1.1.3 imfit

`imfit` is a task in CASA that fits two-dimensional Gaussian models to specified regions of an image. This is useful for quantifying the properties of sources detected in the image. Here's what it does:

Source Fitting Fits Gaussian models to sources in an image to determine their position, shape, and intensity.

Parameter Estimation Provides estimates of parameters such as peak intensity, integrated flux density, position, and shape (major and minor axes, and position angle).

Error Analysis Calculates uncertainties in the fitted parameters, giving a sense of the reliability of the fit.

Multiple Components Can fit multiple Gaussian components if multiple sources are present in the specified region.

1.1.4 imstat

`imstat` is a task in CASA used to compute statistical properties of an image. This helps astronomers understand the basic characteristics of their data. Here's what it does:

Basic Statistics Computes statistics such as mean, median, standard deviation, minimum, maximum, and sum for pixel values within a specified region of the image.

Region Specification Allows users to define the region of interest using various shapes (boxes, circles, polygons) and masks.

Pixel Count Provides the number of pixels within the region and the number of non-zero pixels.

Histogram Optionally generates a histogram of pixel values within the specified region.

1.2 CARTA

CARTA (Cube Analysis and Rendering Tool for Astronomy) is a high-performance visualization tool designed for the interactive analysis of large astronomical datasets, particularly spectral data cubes. It offers a modern, web-based interface, high-performance rendering, and integrated analysis tools, making it an essential tool for astronomers working with large datasets.

1.2.1 Key Features of CARTA

- **Interactive Visualization:** Real-time interaction with large datasets, including 2D images, 3D spectral data cubes, and 4D (time-dependent) data.
- **Performance:** Optimized for high performance using parallel processing and GPU acceleration.
- **User Interface:** Modern web-based interface with tools for zooming, panning, and adjusting contrast and color maps.
- **Analysis Tools:** Integrated tools for spectral line analysis, moment maps, and region statistics.
- **Customization:** Extensible through plugins and scripts with a customizable interface.

2. Work

2.1 Taking a look at the data

(6) The data used is part of a larger data package used for NRAO calibration and imaging tutorials. Taking a look at the data we have:

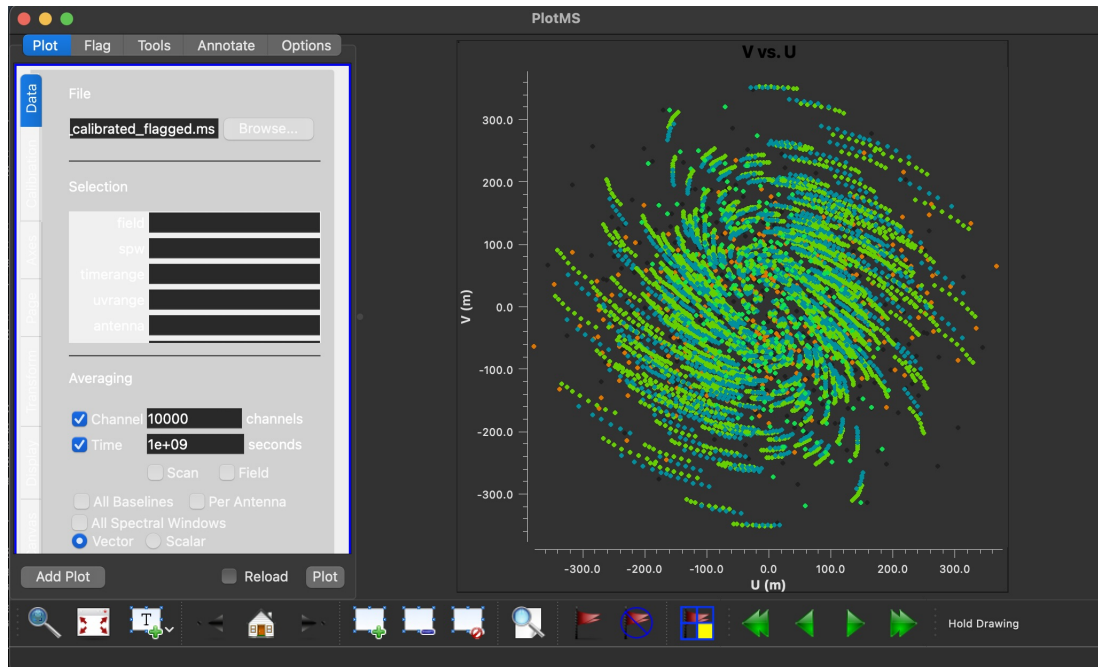


Figure 2.1: UV coverage for the TW Hya data set. The colors in the UV coverage plot identify different observing targets.

2.2 Using tclean

2.2.1 Post cleaning

When `niter` is set to 0/not set, `tclean` does no cleaning. We set `niter` to some larger number, here 5000:

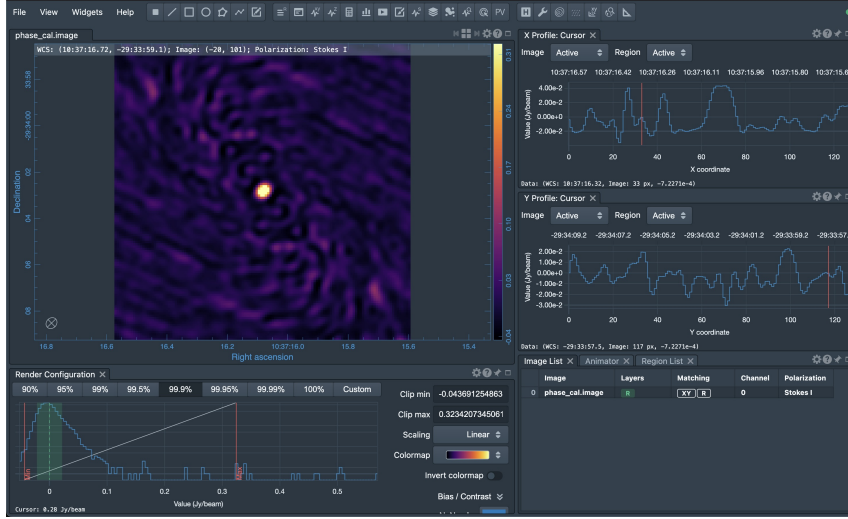


Figure 2.2: `niter` = 5000

2.2.2 Changing weighting scheme

`tclean` includes a lot of options. We can see the list of inputs for the task by typing `inp tclean`. One option that is very commonly tweaked by the user is the weighting scheme used to grid the UV data into a fourier-plane image. This weighting was `robust=0.5` in the first example (by default). We use `tclean` with `briggs` weighting and `robust = -1` and run a few cycles of `tclean`, until you are happy with the level of the residuals:

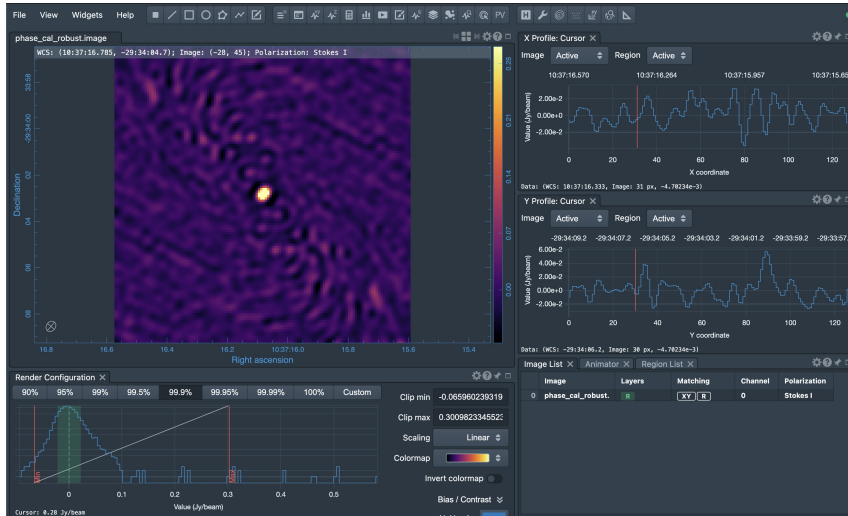


Figure 2.3: using briggs weighting and robust = -1

2.2.3 Tweaking calibrators

Experimenting a bit with `tclean`, try imaging the other calibrators (fields 0 and 2; check the ‘ScanIntent’ again in the `listobs` output) and making the image size and cell size larger and smaller.

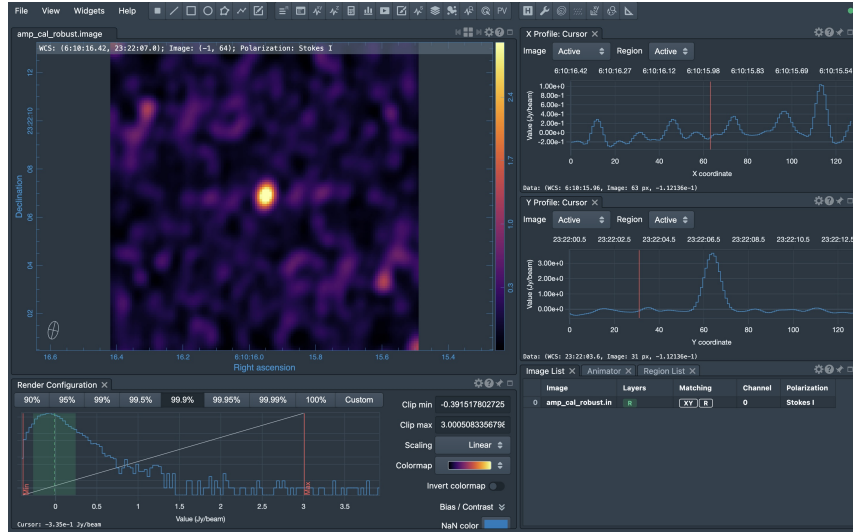


Figure 2.4: field = ’2’

2.2.4 Using big pixel size

If you try a really big pixel size you will see things break. It is recommended to have the pixel size small compared to the synthesized beam for `tclean` purposes (`tclean` quantizes the deconvolution in units of pixels). When the pixel size is big compared to the synthesized beam the imaging in general will degrade, even independent of how you `tclean`.

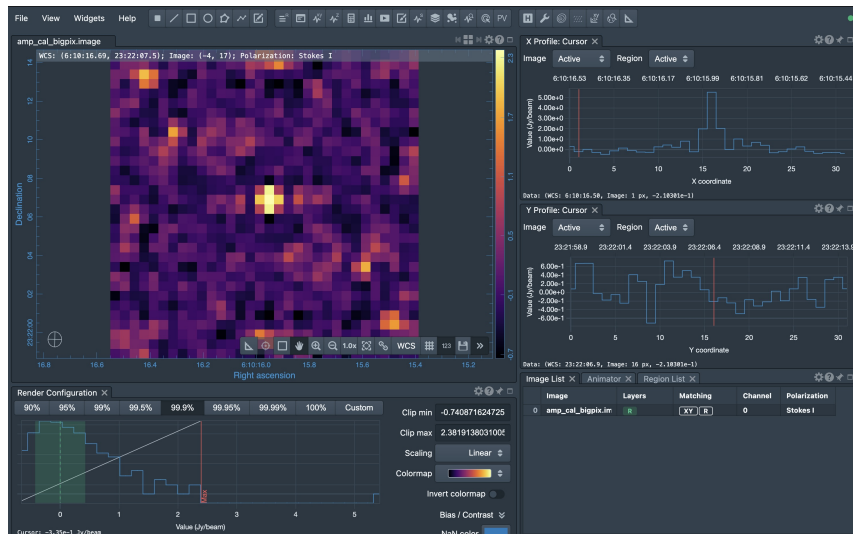


Figure 2.5: `imsize` = (32, 32) instead of (128, 128)



Week6

1	Theory	43
1.1	Introduction to MCMC	
1.2	Key Points	
2	Work	45
2.1	Practice Problems	

1. Theory

1.1 Introduction to MCMC

Data Analysis Recipes: Using Markov Chain Monte Carlo by David W. Hogg and Daniel Foreman-Mackey provides a practical introduction to the use of Markov Chain Monte Carlo (MCMC) methods for data analysis. This document is designed to help scientists and researchers apply MCMC techniques to their work.

1.2 Key Points

1.2.1 Introduction to MCMC

MCMC is a class of algorithms used to sample from probability distributions by constructing a Markov chain. These methods are particularly useful for estimating the posterior distribution in Bayesian inference problems.

1.2.2 Basic Concepts

- **Markov Chain:** A sequence of random variables where the future state depends only on the present state, not on the sequence of events that preceded it.
- **Monte Carlo:** Refers to using random sampling to compute results, often for numerical integration or optimization.

1.2.3 Bayesian Inference

The document emphasizes the use of MCMC in Bayesian inference, where the goal is to update the probability distribution of a hypothesis as more evidence or information becomes available.

- **Posterior Distribution:** The probability distribution representing what we know about the parameters after observing the data.

1.2.4 Common MCMC Algorithms

- **Metropolis-Hastings Algorithm:** A general method for obtaining a sequence of random samples from a probability distribution for which direct sampling is difficult.
- **Gibbs Sampling:** A special case of the Metropolis-Hastings algorithm where sampling is done for each variable conditional on the current values of the other variables.

1.2.5 Practical Implementation

The document provides detailed steps on setting up MCMC simulations, choosing appropriate priors, and diagnosing convergence. Emphasis is placed on practical aspects such as the selection of proposal distributions, burn-in periods, and thinning of samples.

1.2.6 Applications and Examples

Practical examples and recipes for applying MCMC to real-world data analysis problems are provided. Examples include parameter estimation in statistical models, fitting complex models to data, and evaluating uncertainties in model predictions.

1.2.7 Diagnostic Tools

Techniques for assessing the convergence of MCMC chains are discussed, including trace plots, autocorrelation analysis, and the Gelman-Rubin statistic. Common pitfalls and how to avoid them are also covered, ensuring robust and reliable results.

1.2.8 Software and Tools

The document introduces software packages and libraries that facilitate MCMC, such as `emcee` for Python. Guidance on integrating MCMC methods into existing data analysis workflows is provided.



2. Work

The paper *Data Analysis Recipes: Using Markov Chain Monte Carlo* by David W. Hogg and Daniel Foreman-Mackey includes several problems for practice. These problems are designed to help readers apply MCMC methods to a variety of data analysis scenarios, enhancing their understanding and skills in Bayesian inference and MCMC techniques.

2.1 Practice Problems

Problem 1: Parameter Estimation in a Simple Model

Estimate the parameters of a simple linear model $y = mx + b$ given noisy data. Implement an MCMC method to sample the posterior distribution of the slope m and intercept b .

Problem 2: Fitting a Gaussian

Fit a Gaussian function to a set of data points. Use MCMC to estimate the parameters of the Gaussian, including the mean, standard deviation, and amplitude. Evaluate the posterior distributions of these parameters.

Problem 3: Robust Line Fitting

Fit a straight line to data that includes outliers. Implement a robust model using MCMC that accounts for the outliers, perhaps by using a mixture model or a heavy-tailed error distribution.

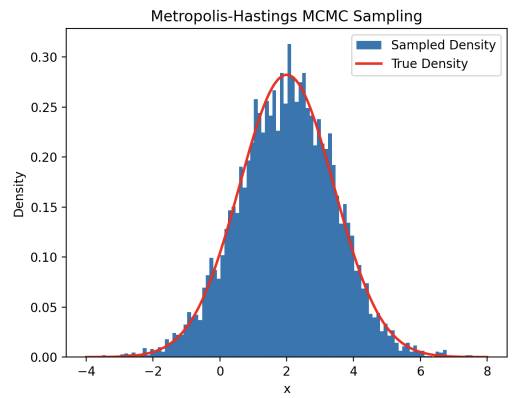


Figure 2.1: Problem 2

Problem 4: Modeling Periodic Data

Model periodic data, such as a time series with a known period but unknown amplitude and phase. Use MCMC to estimate the amplitude, phase, and other relevant parameters.

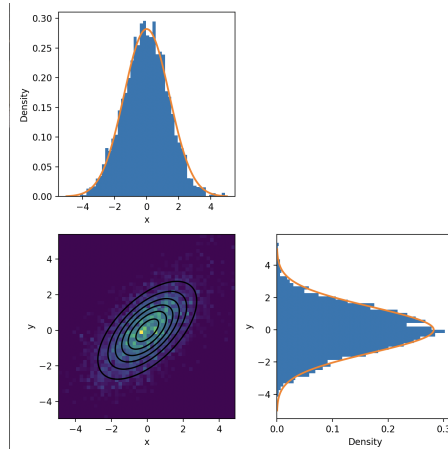


Figure 2.2: Problem 4a

Problem 5: Multimodal Distributions

Explore a posterior distribution with multiple modes. Implement an MCMC algorithm that can effectively sample from a multimodal distribution and identify the different modes.

Problem 6: Hierarchical Models

Construct and sample from a hierarchical Bayesian model. This problem involves estimating parameters at multiple levels, such as individual and group-level parameters, using MCMC.

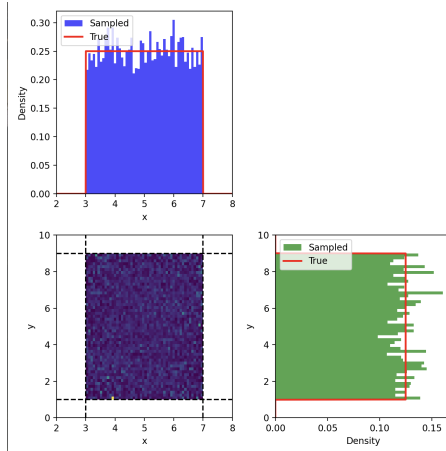


Figure 2.3: Problem 4b

Problem 7: Model Comparison

Perform model comparison using Bayesian methods. Use MCMC to estimate the evidence (marginal likelihood) for different models and compare them to determine the best model for the given data.

Problem 8: Non-Gaussian Likelihoods

Fit a model to data where the likelihood is non-Gaussian, such as Poisson-distributed data. Implement MCMC to sample from the posterior distribution in this scenario.

VI

1	Work	51
1.1	Introduction	
1.2	Initial Implementation: Custom MCMC Sampler	
1.3	Advanced Implementation: Using <code>emcee</code>	
1.4	Conclusion	
1.5	Results	
	Bibliography	55
	Books	
	Books	

1. Work

1.1 Introduction

The objective of this project was to fit a smooth broken power law model to synthetic data using Markov Chain Monte Carlo (MCMC) sampling. We explored two different implementations of the MCMC sampler: a custom implementation and a more advanced approach using the `emcee` Python library.

The smooth broken power law model is given by:

$$F(t, v) = 2^{1/s} \left(\frac{v}{3 \text{ GHz}} \right)^{\beta} F_p \left[\left(\frac{t}{t_p} \right)^{-s\alpha_1} + \left(\frac{t}{t_p} \right)^{-s\alpha_2} \right]^{-1/s}$$

where:

- v is the observing frequency,
- β is the spectral index,
- F_p is the flux density at 3 GHz at the light curve peak,
- t is the time post-merger,
- t_p is the light curve peak time,
- s is the smoothness parameter,
- α_1 and α_2 are the power-law rise and decay slopes, respectively.

1.2 Initial Implementation: Custom MCMC Sampler

1.2.1 Methodology

- (a) **Model Definition:** The model was defined using the provided formula, incorporating the natural logarithm of time to ensure numerical stability.

- (b) **Likelihood Function:** The likelihood function was defined based on the Gaussian error model, considering the difference between the observed and model-predicted values.
- (c) **Prior Distribution:** Gaussian priors were applied to all parameters, ensuring they remained within realistic bounds.
- (d) **Metropolis-Hastings Algorithm:** The Metropolis-Hastings (M-H) algorithm was implemented to sample from the posterior distribution of the parameters. The proposal distribution was set as a Gaussian in the natural logarithm of the parameter space.
- (e) **Parameter Initialization:** Initial parameter values were selected, and the sampler was run for a significant number of steps to achieve convergence.
- (f) **Diagnostic and Plots:** Histograms and trace plots were generated to evaluate the convergence and distribution of the sampled parameters.

1.2.2 Challenges

- **Convergence Issues:** Initial runs showed poor convergence, indicating potential issues with parameter initialization and step sizes.
- **Burn-in Period:** Insufficient burn-in periods led to non-stationary samples.

1.3 Advanced Implementation: Using `emcee`

1.3.1 Methodology

- (a) **Model and Likelihood Definition:** The model and likelihood functions were defined similarly to the custom implementation, utilizing logarithmic transformation for stability.
- (b) **Priors:** Priors were explicitly defined for each parameter, ensuring they were realistic and constrained.
- (c) **Ensemble Sampler Initialization:** The `emcee` library's `EnsembleSampler` was used to initialize multiple walkers, ensuring a diverse exploration of the parameter space.
- (d) **Burn-In and Sampling:** A significant burn-in period was included before the main sampling to ensure the chains reached the stationary distribution.
- (e) **Diagnostics:** Trace plots and corner plots were generated to visualize the evolution and distribution of the parameters. Convergence diagnostics were carefully monitored.

1.3.2 Challenges and Improvements

- **Walker Initialization:** Improved initialization by spreading walkers in a Gaussian ball around the initial guess.
- **Extended Burn-In Period:** Increased the burn-in period significantly to allow better convergence.
- **Trace Plot Analysis:** Detailed trace plots were used to ensure each parameter chain mixed well and converged to a stationary

distribution.

- **Increased Step Count:** Extended the total number of steps to ensure thorough exploration of the parameter space.

1.3.3 Outcomes

The initial model gave some good results, but the use of `emcee` resulted in better convergence and more reliable parameter estimates. The diagnostics confirmed that the chains mixed well and converged properly. The posterior distributions were well-defined, and the model fit the data accurately. (5)

1.4 Conclusion

Implementing an MCMC sampler for fitting a smooth broken power law model involved several iterations and improvements. The initial custom MCMC implementation provided valuable insights but faced challenges with convergence and parameter initialization. The advanced implementation using `emcee` addressed these challenges by leveraging the ensemble sampling approach, improved initialization strategies, and extended burn-in periods. This approach resulted in more reliable and robust parameter estimates, demonstrating the effectiveness of using specialized MCMC libraries for complex model fitting tasks.

1.5 Results

The final graph from custom implementation was as follows:

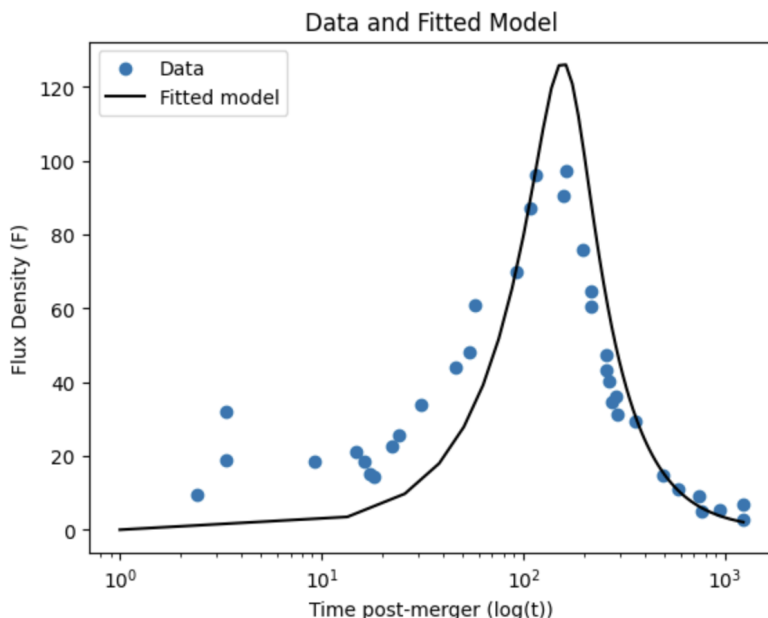


Figure 1.1: Curve fit using Custom Implementation of MCMC

The final graph using emcee was as follows:

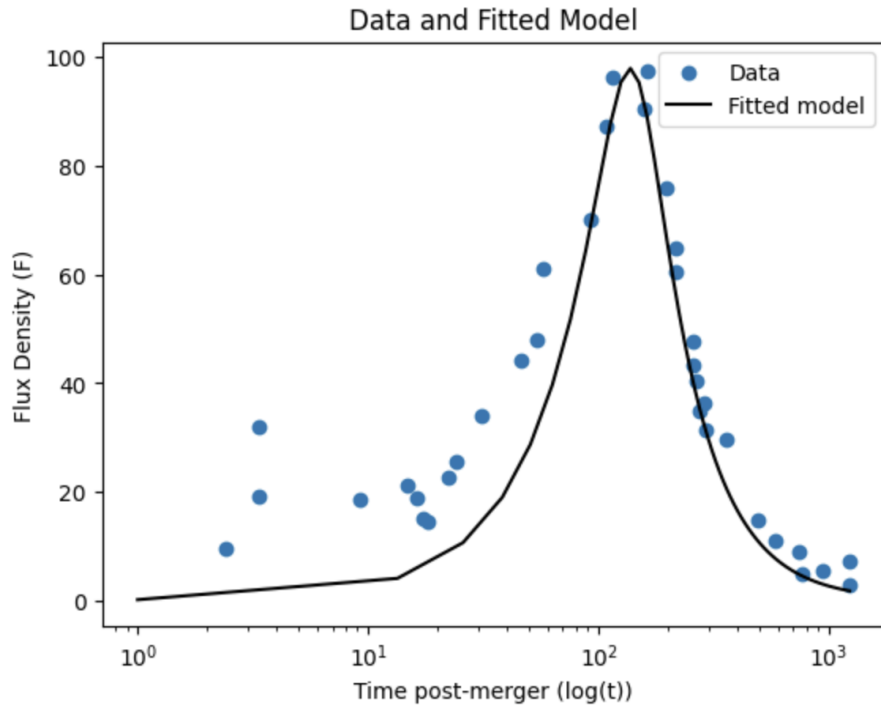


Figure 1.2: Curve fit using emcee of MCMC

Bibliography

Books

- (MSK16a) Jonathan M. Marr, Ronald L. Snell, and Stanley E. Kurtz. *FUNDAMENTALS OF RADIO ASTRONOMY: Observational Methods*. 1st edition. CRC Press, 2016, pages 2–27 (cited on page 9).
- (MSK16b) Jonathan M. Marr, Ronald L. Snell, and Stanley E. Kurtz. *FUNDAMENTALS OF RADIO ASTRONOMY: Observational Methods*. 1st edition. CRC Press, 2016, pages 31–70 (cited on page 17).
- (MSK16c) Jonathan M. Marr, Ronald L. Snell, and Stanley E. Kurtz. *FUNDAMENTALS OF RADIO ASTRONOMY: Observational Methods*. 1st edition. CRC Press, 2016, pages 76–93 (cited on page 27).
- (MSK16d) Jonathan M. Marr, Ronald L. Snell, and Stanley E. Kurtz. *FUNDAMENTALS OF RADIO ASTRONOMY: Observational Methods*. 1st edition. CRC Press, 2016, pages 102–107 (cited on page 29).

Links

- (Cal24) CalTech. http://www.tauceti.caltech.edu/kunal/gw170817/gw170817_afterglow_data_full.txt, Accessed = 2024-05-26. 2024 (cited on pages 13, 53).
- (CAS24) CASA. https://casaguides.nrao.edu/index.php?title=First_Look_at_Imaging_CASA_6.4, Accessed = 2024-07-10. 2024 (cited on page 37).

- (CIR24) CIRADA. http://cutouts.cirada.ca/get_cutout/, Accessed = 2024-05-25. 2024 (cited on page 13).
- (Rag24) Ragolu. <https://ragolu.science.ru.nl/hcat.html>, Accessed = 2024-05-25. 2024 (cited on page 13).